Dalton Transactions

RSC Publishing

PAPER

View Article Online
View Journal | View Issue

Cite this: *Dalton Trans.*, 2013, **42**, 5860

Long-range and short-range orderings in $K_4Fe_4P_5O_{20}$ with a natrolite-like framework

Zhangzhen He,*[a] Weilong Zhang,[a] Wendan Cheng,[a] Atsushi Okazawa[b] and Norimichi Kojima[b]

Received 4th December 2012,
Accepted 3rd February 2013

DOI: 10.1039/c3dt32897j

www.rsc.org/dalton

$K_4Fe_4P_5O_{20}$ shows an interesting natrolite-like structure with a spin–tetrahedron lattice built by mixed valence Fe ions. Single crystals of the title compound are successfully grown by the flux method using KF as flux. Magnetic results combined from magnetic, heat capacity, and ^{57}Fe Mössbauer spectra measurements show that $K_4Fe_4P_5O_{20}$ possesses a short-range magnetic ordering at ~13 K and a long-range ordering at ~7 K. Magnetic anisotropy of $K_4Fe_4P_5O_{20}$ is observed between $H\|c$ and $H\perp c$, suggesting that the *c*-axis is the magnetic easy-axis. The spin arrangements in the system are suggested to be ferrimagnetic along the natrolite chains.

Introduction

The search for new transition metal based oxides has been one of the most active fields in solid state chemistry and physics, due to the discovery of various interesting magnetic phenomena. It is well-known that the magnetic properties of solid magnets are related strongly to their structural features. The compounds with a layer or chain structure are usually found to display low-dimensional quantum magnetic properties,[1] while ones with a triangular or tetrahedral spin lattice are found to exhibit geometrically frustrated spin-glass behavior in general.[2]

Natrolite ($Na_2Al_2Si_3O_{10}\cdot 2H_2O$) is one of the most famous naturally occurring zeolite compounds, composed of SiO_4 and AlO_4 tetrahedra and the unique chemical and structural characteristics have attracted much attention.[3–13] To explore new transition metal based oxides and to further investigate interesting magnetic phenomena, our current interest is focused on natrolite-like compounds obtained through a substitution of transition-metal magnetic ions for nonmagnetic Si or Al elements of $Na_2Al_2Si_3O_{10}\cdot 2H_2O$. Based on this idea, we have recently synthesized a new natrolite-like compound $K_4Fe_4P_5O_{20}$ by high-temperature solid state reaction.[14] Since $K_4Fe_4P_5O_{20}$ is the first natrolite-like compound containing transition-metal magnetic ions, this provides a nice chance to investigate the magnetic behavior of such unique systems. Herein, we report on the low-temperature magnetic behavior of $K_4Fe_4P_5O_{20}$. Our results show that $K_4Fe_4P_5O_{20}$ exhibits an interesting spin-tetrahedron lattice, in which long-range and short-range orderings occur at low-temperature. A spin frustration effect is also confirmed in the title material. To the best of our knowledge, it is first time to suggest that transition-metal based oxides with a natrolite-like structure may be considered as geometrically frustrated spin systems.

Experimental section

Single crystals of $K_4Fe_4P_5O_{20}$ were grown by flux method using a mixture of high purity reagents of K_2CO_3 (6.9 g), Fe_2O_3 (16 g), $NH_4H_2PO_4$ (23 g), and KF (5.8 g) in an alumina crucible ($\Phi 42 \times 50$ mm^3). The quality of the single crystals was confirmed by X-ray powder diffraction (XRD) technique, which was performed at room temperature in the range $2\theta = 10°–80°$ with a scan step width of 0.02° and a fixed counting time of 4 s using an MXP21AHF (Mac Science) powder diffractometer with graphite monochromatized CuKα radiation. The directions of the surface of crystals were determined using a Bruker SMART three-circle diffractometer equipped with a CCD area detector. Magnetic and heat capacity measurements were performed using a commercial Quantum Design Physical Property Measurement System (PPMS). The ground single-crystal sample (~30.5 mg) was placed in a gel capsule sample holder suspended in a plastic drinking straw. Magnetic susceptibility was measured at 0.1 T from 300 to 2 K (temperature scan of 2 K min^{-1}) and magnetization was measured at 2 K in an applied field from −8 to 8 T (field scan of 0.01 T per step). Heat capacity was measured at zero field by a relaxation method using a pellet sample (2.5 × 2.5 mm^2, ~10.2 mg). A bunch of single crystals (15.6 mg) were selected for magnetic anisotropy measurements. The crystal was stuck horizontally

[a]*State Key Laboratory of Structural Chemistry, Fujian Institute of Research on the Structure of Matter, Chinese Academy of Sciences, Fuzhou, Fujian 350002, China. E-mail: hezz@fjirsm.ac.cn*
[b]*Graduate School of Arts and Sciences, University of Tokyo, Komaba 3-8-1, Meguro, Tokyo 153-8902, Japan*

Table 1 Mössbauer spectral parameters for $K_4Fe_4P_5O_{20}$ at different temperatures

Site	T (K)	δ (mm s^{-1})	Δ (mm s^{-1})	Γ (mm s^{-1})	% (mm s^{-1})	H (T)
Doublet (1)	300	0.511(7)	0.624(10)	0.588(17)	76.0	
Doublet (2)		1.27(3)	2.65(6)	0.59(fixed)	24.0	
Doublet (1)	13	0.550(5)	0.696(8)	0.794(16)	75.7	
Doublet (2)		1.22(2)	2.77(4)	0.79(fixed)	24.3	
Doublet (1)	10	0.55(2)	1.20(4)	0.99(8)	9.7	
Magnetic (1)		0.41(11)		1.4(4)	5.5	21.6(6)
Singlet (1)		0.84(6)		10.7(8)	84.8	
Doublet (1)	6	0.69(2)	1.97(4)	0.89(7)	12.2	
Magnetic (1)		0.71(4)		1.54(13)	32.3	26.2(3)
Magnetic (2)		0.46(4)		1.3(4)	27.0	47.8(5)
Magnetic (3)		0.41(4)		1.6(3)	28.6	40.9(8)
Doublet (1)	3.7	0.61(2)	2.20(4)	0.66(6)	7.6	
Magnetic (1)		0.69(4)		1.25(12)	18.7	27.4(3)
Magnetic (2)		0.475(13)		0.84(9)	29.1	49.85(16)
Magnetic (3)		0.46(2)		1.68(11)	44.6	44.0(5)

and vertically in a plastic drinking straw using flame retardant tape. The measured conditions of dc magnetization are similar to those for the ground single-crystal sample. The Mössbauer spectra were measured from 300 to 3.7 K with a constant acceleration spectrometer using a rhodium matrix cobalt-57 source at room temperature in the transmission geometry. The spectra were calibrated by using the six lines of a body-centred cubic iron foil (α-Fe) and were fitted by a Lorentzian function, the centre of which was taken as zero isomer shift. The hyperfine parameters are provided in Table 1.

Results and discussion

Crystal structure and spin lattice

$K_4Fe_4P_5O_{20}$ crystallizes in the tetragonal space group $P\bar{4}2c$ with a = 9.7450(7) Å, c = 9.3800(9) Å, and Z = 2.[14] There are one K atom, one Fe atom, and two P atoms in the asymmetric unit. As shown in Fig. 1, the Fe atoms are coordinated by five oxygen atoms, forming a trigonal-bipyramid with Fe–O bond lengths ranging from 1.903(6) to 1.984(5) Å. P atoms have two different sites, P^I and P^{II}, which are tetrahedrally coordinated by four oxygen atoms, forming a distorted P^IO_4 tetrahedron with P^I–O bond lengths ranging from 1.528(3) to 1.558(3) Å and a regular $P^{II}O_4$ tetrahedron with P^{II}–O bond lengths of 1.527(1) Å, respectively. K atoms are surrounded by ten oxygen atoms with K–O bond lengths ranging from 2.739(6) to 3.418(6) Å.

As shown in Fig. 2, the three-dimensional (3D) framework of $\{Fe_4P_5O_{20}\}_\infty$ is built up from FeO_5 and PO_4, in which FeO_5 trigonal bipyramids are linked with P^IO_4 tetrahedra to each other *via* a corner-sharing oxygen atom to form a unit cluster $[Fe_4P^I{}_4O_{16}]$. The clusters are further connected with $P^{II}O_4$ tetrahedra to form one-dimensional linear chains running along the c-axis. The chains are linked to each other through a corner-shared FeO_5-to-P^IO_4 manner to form eight-column elliptic tunnels, in which potassium ions are located. Such a structural feature was found to be quite similar to that of natrolite $Na_2Al_2Si_3O_{10}\cdot 2H_2O$.[14] However, we note that both FeO_5 and PO_4 are isolated in the framework of $\{Fe_4P_5O_{20}\}_\infty$, which is obviously different from AlO_4 and SiO_4 in the natrolite family. Since K^+ ions and PO_4 groups are nonmagnetic, the spin lattices in $K_4Fe_4P_5O_{20}$ are determined by the arrangements of magnetic Fe ions. Removing PO_4 groups from the structural unit $\{Fe_4P_5O_{20}\}$, four Fe ions form a distorted tetrahedral spin lattice with two different distances between Fe

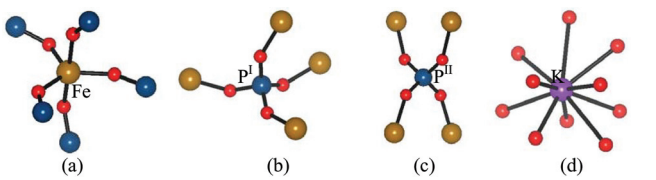

Fig. 1 The oxygen-coordination environments for (a) Fe, (b) P1, (c) P2, and (d) K atoms, respectively.

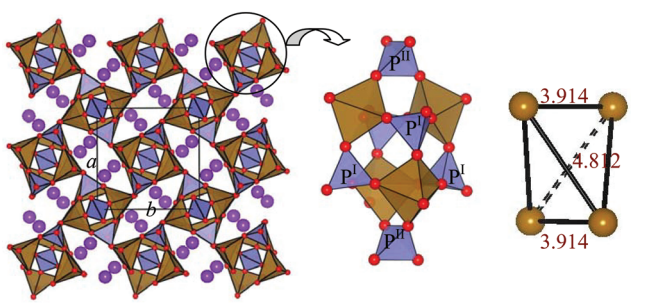

Fig. 2 The crystal structure of $K_4Fe_4P_5O_{20}$ viewed on the a–b plane, where brown polyhedra, blue tetrahedra, purple balls, and red balls represent the FeO_5, PO_4, K, and O, respectively. The circle shows a basic structural unit of $\{Fe_4P_5O_{20}\}$, which corresponds to a distorted tetrahedron lattice with different bond distances (Å).

ions [3.91(4) and 4.81(2) Å]. It is noted that Fe_4 spin units of the structural unit $\{Fe_4P_5O_{20}\}$ may also be considered as a cluster in distorted tetrahedral spin lattices.

Crystal growth

Single crystals of $K_4Fe_4P_5O_{20}$ were grown in a closed alumina crucible by the flux method using KF as flux. As shown in Fig. 3, $K_4Fe_4P_5O_{20}$ crystals show a needle growth behavior and a fibrous morphology. The crushed single crystals were checked by X-ray powder diffraction technique in Fig. 4, confirming there are no impurity phases. This suggests that the grown crystals are of high quality. It must be noted that $K_4Fe_4P_5O_{20}$ crystals cannot be grown directly from the mixture of K_2CO_3, Fe_2O_3 and $NH_4H_2PO_4$ as starting materials owing to the large viscosity of the solution. Although we have tried by changing the molar ratio of the starting materials, amorphous solidifications were obtained in the end with cooling of the solution. Thus KF is considered to play an important role in flux or mineralization for this growth process. In addition, there are some important points for this growth of $K_4Fe_4P_5O_{20}$: to prevent inclusions of the melt into the crystal due to overcooling of the melt, the furnace was kept at a constant temperature several times in the cooling process. Also, since

Fig. 3 Single crystals of $K_4Fe_4P_5O_{20}$ with a needle growth behavior and a fibrous morphology.

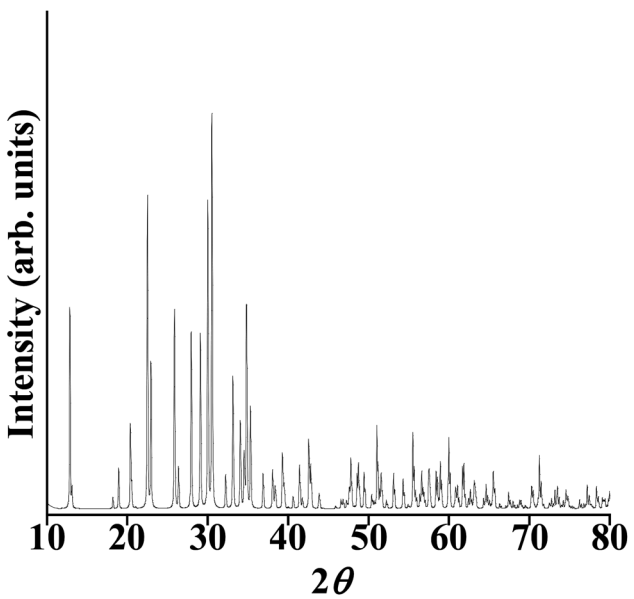

Fig. 4 A typical powder XRD pattern of $K_4Fe_4P_5O_{20}$.

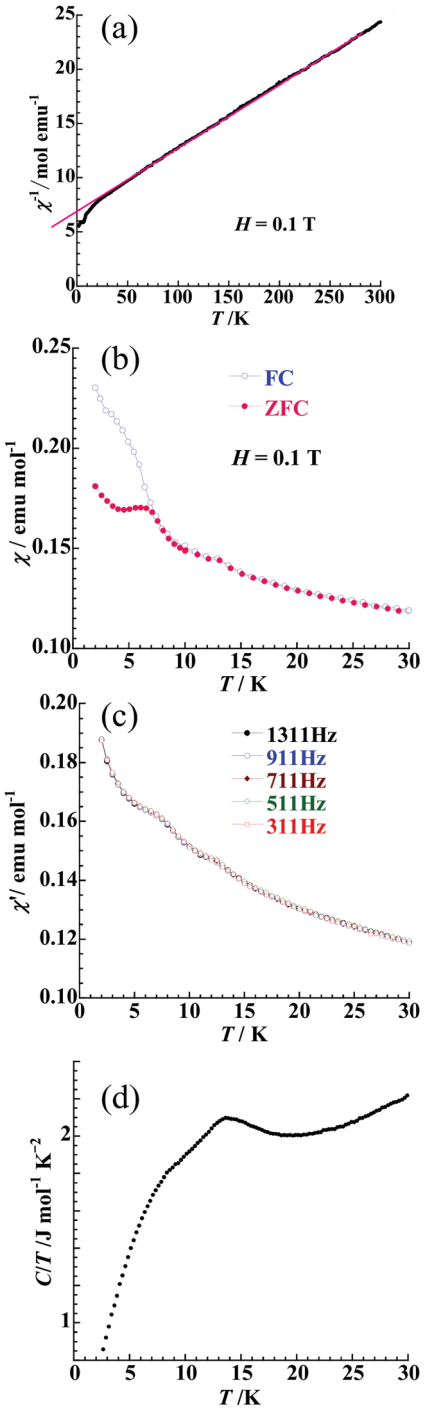

Fig. 5 (a) The temperature dependence of the reciprocal susceptibility measured in an applied field of 0.1 T. (b) dc magnetic susceptibilities obtained in the field cooled and zero field cooled regimes. (c) The ac susceptibilities measured at different frequencies. (d) The heat capacity data measured at zero field.

$K_4Fe_4P_5O_{20}$ exhibits mixed valence with Fe^{2+} and Fe^{3+} ions, it is necessary to keep the reducing gas NH_3, arising from the decomposition of $NH_4H_2PO_4$, in the crucible. Thus, the alumina crucible was capped with a cover using Al_2O_3 cement to be a closed system in the growth process.

Magnetic properties

Fig. 5a demonstrates the temperature dependence of the magnetic susceptibility of a polycrystalline sample. A typical Curie–Weiss behavior is observed above 30 K, giving the Curie constant C = 16.5(3) emu K mol^{-1} and Weiss constant θ = −107(1) K. The effective magnetic moment (μ_{eff}) is calculated to be 5.75(1) μ_B, which is larger than the value of 4.899 μ_B for S = 2 (high spin state of Fe^{2+} ions) and smaller than that of 5.916 μ_B for S = 5/2 (high spin state of Fe^{3+} ions) with a g factor of 2, showing the mixed valence of Fe^{2+}/Fe^{3+} in the system.

The low-temperature magnetic behavior was confirmed by dc magnetic susceptibilities obtained in the field cooled (FC) and zero field cooled (ZFC) regimes (Fig. 5b). A broad peak is observed at ~13 K, showing the onset of short-range ordering. The rapid increase of susceptibility starts at ~9 K and the magnetic susceptibility for ZFC deviates from that for FC below ~7 K, indicating the appearance of long-range ordering. Such successive magnetic transitions are also observed by ac magnetic susceptibilities measured at different frequencies (Fig. 5c), clearly showing two anomalies at ~7 and ~13 K, respectively. The peak temperatures are independent of frequency, suggesting that the magnetic transitions are not of spin-glass freezing but antiferromagnetic ordering. As shown in Fig. 5d, heat capacity data give a clear evidence for two magnetic transitions, in which a broad peak is observed at ~13 K while a shoulder anomaly is observed at ~7 K.

To confirm the magnetic anisotropy, magnetic measurements were also done at a magnetic field parallel and perpendicular to the c-axis of $K_4Fe_4P_5O_{20}$. As shown in Fig. 6a, the diversity of susceptibilities is clearly observed below 13 K between $H\|c$ and $H\perp c$, showing the appearance of magnetic anisotropy at low temperature. Furthermore, the rapid upturn of susceptibility below 10 K and a clear peak at ~13 K can be seen at $H\|c$, indicating that the c-axis may be the magnetic easy-axis. Fig. 6b shows magnetization (M) as a function of applied field (H) at T = 2 K. A nonlinear increase in magnetization is observed and magnetization does not saturate even in 8 T for both $H\|c$ and $H\perp c$. However, a clear hysteresis and remanent magnetization near H = 0 are observed for $H\|c$, while nothing is observed for $H\perp c$, supporting the unusual magnetic anisotropy in the system. Moreover, considering that the Weiss constant θ obtained from the susceptibility is negative and the magnetic Fe ions exhibit mixed valence of Fe^{2+} and Fe^{3+}, the M–H curve may indicate a ferrimagnetic spin arrangement along the c-axis.

To further identify the nature of magnetic behavior of $K_4Fe_4P_5O_{20}$, ^{57}Fe Mössbauer spectra were measured from room temperature to 3.7 K (Fig. 7). At the temperature range of 300–13 K the spectra consist of paramagnetic doublets, which are assigned to high-spin Fe^{3+} (isomer shift of ~0.5 mm s^{-1}) and Fe^{2+} ions (that of ~1.3 mm s^{-1}).[15] This is concrete evidence for mixed valence Fe ions in the system. Furthermore, the area ratio of the two doublets (Fe^{3+} : Fe^{2+}) is about 76 : 24 (as seen in Table 1), agreeing with the occupation of 3/4 Fe^{3+} and 1/4 Fe^{2+} ions in the $Fe_4P_5O_{20}$ units that is suggested by structural analysis.[14] With decreasing the temperature, a broadened Mössbauer spectrum is observed at around 10 K. Such a broad component indicates the appearance of short-range ordering. The Zeeman splitting to a magnetic sextuplet is observed at 7 K and below, showing long-range magnetic ordering. The hyperfine field is ~50 T at 3.7 K. We note that the Mössbauer data are in good agreement with magnetic and heat capacity data, confirming the mixed valence Fe^{2+}/Fe^{3+} ions in the system and further supporting the appearance of long-range and short-range orderings at low temperature.

The above results combined from susceptibility, magnetization, heat capacity, and ^{57}Fe Mössbauer spectra measurements confirmed that $K_4Fe_4P_5O_{20}$ possesses a short-range ordering at

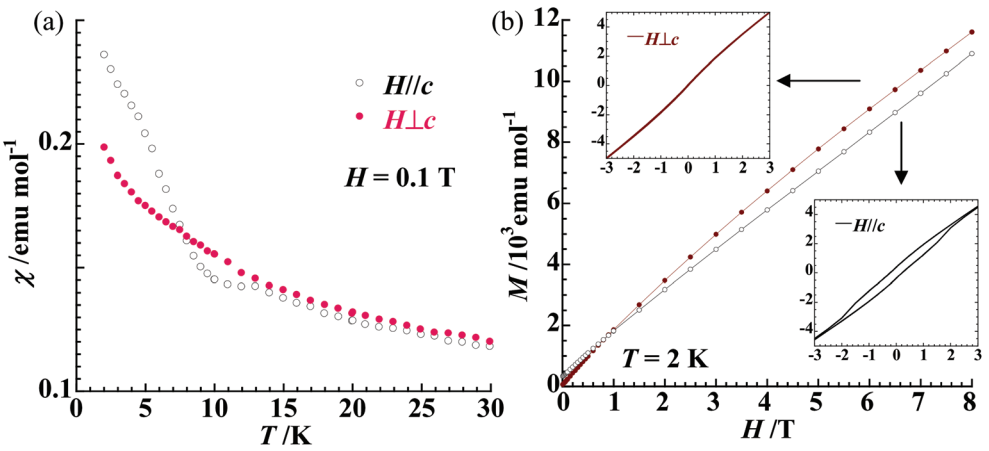

Fig. 6 (a) The temperature dependence of the magnetic susceptibility measured in a magnetic field parallel and perpendicular to the c-axis of single crystals. (b) Isothermal magnetization *versus* magnetic field curves at 2 K. The inset shows a different hysteresis between $H\|c$ and $H\perp c$.

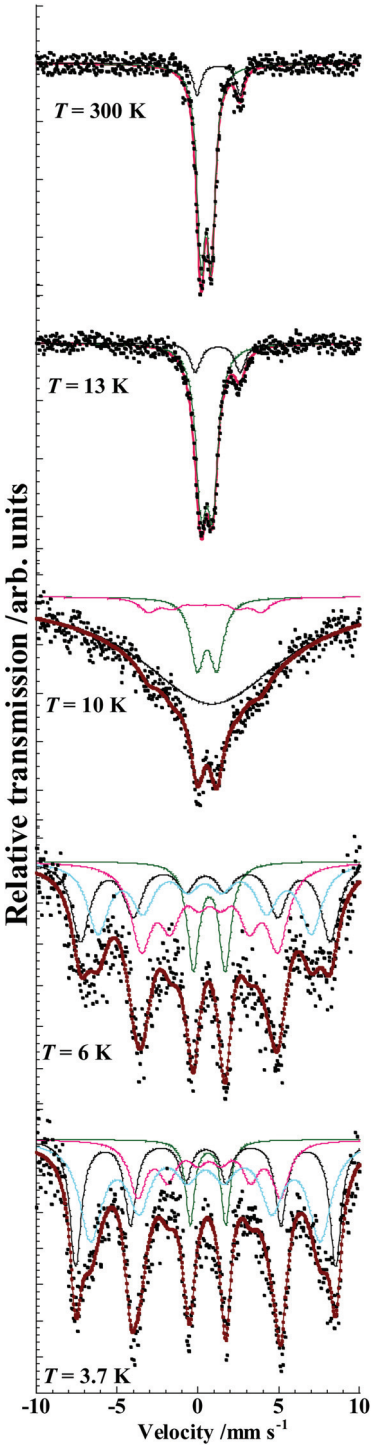

Fig. 7 The Mössbauer spectra measured from 300 to 3.7 K, where the circles are experimental data and the lines are the fits using a Lorentzian function.

~13 K and a long-range ordering at ~7 K. Since all of the Fe ions for the titled material exhibit mixed valence of Fe^{3+}/Fe^{2+} with the ratio of 3 : 1 in the same crystallographic site, the magnetic ground state seems to be a long-range ferrimagnetic ordering. We suggest that a long-range ordering at low temperature may be due to non-equivalent interaction exchanges between mixed valence Fe ions (Fe^{3+} and Fe^{2+}) in Fe_4 clusters, although an isosceles spin–tetrahedron lattice looks likely to show a geometrical frustration effect. Also, we note that the *c*-axis of $K_4Fe_4P_5O_{20}$ is the magnetic easy axis, indicating that the spins are arranged parallelly along the *c*-axis. Furthermore, we suggest that multiple magnetic transitions in $K_4Fe_4P_5O_{20}$ may arise from the competition of multiple interaction exchanges between Fe_4 spin-clusters in the framework. To judge spin frustration in tetrahedral Fe_4 spin lattices, an empirical measure is suggested by defining the value of $f = |\theta_{CW}|/T_c$, where θ_{CW} is the Weiss temperature, and T_c is an ordering temperature. The value of $f > 10$ indicates a strong frustration effect in magnetic systems.[16] The value of $f = 15$ ($\theta = \sim 107$ K, $T_c = \sim 7$ K) is obtained for $K_4Fe_4P_5O_{20}$, confirming the appearance of a geometrical frustration effect. The result suggests that transition-metal oxides with a natrolite-like structure may be considered as geometrically frustrated spin systems.

Conclusion

A new natrolite-like compound $K_4Fe_4P_5O_{20}$ shows an interesting 3D distorted tetrahedral spin lattice, which is built by magnetic trigonal-bipyramidal FeO_5 units. Single crystals of the title compound were grown by the flux method using KF as flux in a closed alumina crucible. Magnetic results combined from magnetic, heat capacity, and ^{57}Fe Mössbauer spectra measurements confirmed that $K_4Fe_4P_5O_{20}$ possesses a short-range magnetic ordering at ~13 K and a long-range ordering at ~7 K. The slight magnetic anisotropy was observed between $H \| c$ and $H \perp c$, suggesting that the *c*-axis is the magnetic easy-axis. Considering that the Weiss constant θ is negative and magnetic Fe ions exhibit mixed valence consisting of Fe^{2+} and Fe^{3+}, the spin arrangement in the system seems to be ferrimagnetic type along the natrolite chains of $K_4Fe_4P_5O_{20}$. Also, a strong geometrical frustration effect was obtained in the system due to distorted tetrahedral spin lattice.

Acknowledgements

This work was financially supported by the NSFC (grant no. 11074250), the National Basic Research Program of China (no. 2012CB921701), the NSF of Fujian Province (2010J01019), and Program for Excellent Talents in Fujian Province.

References

1 P. Lemmens, G. Guntherodt and C. Gros, *Phys. Rep.*, 2003, **375**, 1.
2 J. E. Greedan, *J. Mater. Chem.*, 2001, **11**, 37.
3 L. Pauling, *Proc. Natl. Acad. Sci. U. S. A*, 1930, **16**, 453.
4 E. Stuckenschmidt, W. Joswig and W. H. Baur, *Phys. Chem. Miner.*, 1994, **21**, 309.

5 N. E. Ghermani, C. Lecomte and Y. Dusausoy, *Phys. Rev. B: Condens. Matter*, 1996, **53**, 5231.
6 Y. Lee, J. A. Hriljac, S. J. Kim, J. C. Hanson and T. Vogt, *J. Am. Chem. Soc.*, 2003, **125**, 6036.
7 Y. Lee, S. J. Kim, C.-C. Kao and T. Vogt, *J. Am. Chem. Soc.*, 2009, **131**, 7554.
8 Y. Lee, T. Vogt, J. A. Hriljac, J. B. Parise and G. Artioli, *J. Am. Chem. Soc.*, 2002, **124**, 5466.
9 Y. Lee, T. Vogt, J. A. Hriljac, J. B. Parise, J. C. Hanson and S. J. Kim, *Nature*, 2002, **420**, 485.
10 Y. Lee, Y. Lee and D. Seoung, *Am. Mineral.*, 2010, **95**, 1636.
11 J. Shin, D. S. Bhange, M. A. Camblor, Y. Lee, W. J. Kim, I.-S. Nam and S. B. Hong, *J. Am. Chem. Soc.*, 2011, **133**, 10587.
12 G. L. Hill, E. Bailey, M. C. Stennett, N. C. Hyatt, E. M. Maddrell, P. F. McMillan and J. A. Hriljac, *J. Am. Chem. Soc.*, 2011, **133**, 13883.
13 Y. Lee, D. Liu, D. Seoung, Z. Liu, C.-C. Kao and T. Vogt, *J. Am. Chem. Soc.*, 2011, **133**, 1674.
14 Z. He, W. Zhang, W. Cheng, A. Okazawa and N. Kojima, *Inorg. Chem.*, 2012, **51**, 7469.
15 R. P. Hermann, F. Hatert, A.-M. Fransolet, G. L. Long and F. Grandjean, *Solid State Sci.*, 2002, **4**, 507.
16 A. P. Ramirez, *Annu. Rev. Mater. Sci.*, 1994, **24**, 453.